RSC Advances

ROYAL SOCIETY OF CHEMISTRY

www.rsc.org/advances

RSC Advances
CREATED USING THE RSC ARTICLE TEMPLATE (VER. 3.1) - SEE WWW.RSC.ORG/ELECTRONICFILES FOR DETAILS
ARTICLE TYPE www.rsc.org/xxxxxx | XXXXXXXX

A facile synthesis of ZnO/CNTs hierarchical mircosphere composites with enhanced photocatalytic degradation of methylene blue

Guang Zhu[1,*], Hongyan Wang[1], Gaoxia Yang[1], Liangwei Chen[1], Peijun Guo[2], Li Zhang[1,*]

Received (in XXX, XXX) Xth XXXXXXXXX 200X, Accepted Xth XXXXXXXXX 200X
First published on the web Xth XXXXXXXXX 200X
DOI: 10.1039/b000000x

Novel carbon nanotubes (CNTs) and hierarchical ZnO mircosphere composites were prepared via a facile chemical deposition route and their photocatalytic performance in degradation of methylene bule (MB) was investigated. The results indicate that as-prepared ZnO/CNTs hierarchical microsphere composite with 1.1 wt% CNTs shows the optimized photocatalytic activity. The photocatalytic performance improvement can be attributed to the triple effects of high surface area, enhanced light absorption and suppression of charge carriers recombination resulting from the interaction between ZnO and CNTs.

1. Introduction

Photocatalytic degradation of organic pollutants from waste water has engrossed wide attention due to its efficiency, easy operation and preferably producing nontoxic end products.[1–8] The photocatalysis mechanism is as follows: the electrons are excited from the valence band (VB) of semiconductors to the conduction band (CB) and form electron−hole pairs under UV or visible light irradiation.[9-12] These electrons and holes can migrate and initiate redox reactions with water and oxygen, leading to the formation of a variety of reactive oxidation species, which can oxidize the organic compounds. However, the quick recombination of photo-generated electrons and holes can significantly decrease the photocatalytic performance.[13-15] Therefore, a number of efforts have been attracted to inhibit the recombination of electron-hole pairs and improve charge transport. So far, other materials doped the wide band gap semiconductor photocatalysts as one effective method has been widely researched to address the above problem and improve photocatalytic performance, such as quantum dots,[16,17] Au,[18-20] Ag,[21,22] nitrogen,[23] fullerene,[24] and so on.

Carbon nanotubes (CNTs), an important member in carbon family, has potential applications in photocatalysis, energy storage, solar cells, and transparent electrodes due to their low cost, large surface area, superior chemical stability, and good catalytic activity.[25-29] Recently, many works have demonstrated that CNTs incorporated with metal oxide semiconductor, show high activity for photocatalytic applications.[30-35] The enhanced performance can be attributed to the improved electron transfer from the conduction band of semiconductor to the CNTs in the process of photocatalysis.[36-38] Among metal oxide semiconductor catalysts, ZnO has been getting increased attention due to its suitable band gap of 3.37 eV and high electron mobility of 115-155 $cm^{-2}V^{-1}S^{-1}$.[39,40] So far, a few publications focus on the research of the CNTs doped ZnO composites and show a enhanced photocatalytic performance. Ahmad et al. prepared ZnO/CNTs nanocomposite by using sol method and used as-prepared nanocomposites as catalysts to photodegrade RhB dye.[31] The results indicated that ZnO/CNTs nanocomposite has a superior photodegradation efficiency of RhB in comparison with the pure ZnO nanoparticle due to enhanced the electron-holes separation at the hetero-interface. Lv et al. reported that the ZnO/RGO/CNTs were prepared by microwave assisted method and used to photodegrade methylene blue (MB), and a degradation efficiency of 96% was achieved under UV light irradiation.[41] Gao et al. prepared ZnO nanoparticles coated multi-walled carbon nanotubes for the photocatalytic degradation of MB, and results indicated that as-prepared composites have a higher photocatalytic activity than ZnO bulk material or the mechanical mixture of MWCNTs and ZnO.[42] Despite the above progress to date, as promising hybrid materials for photocatalysis, the exploration on ZnO-CNTs composites is not nearly enough so far. It is well known that the photocatalytic performance strongly depends on the morphology of materials. Recently, hierarchically structured ZnO has been fabricated and used to enhance photocatalytic performance due to large surface area and higher electron transport of organic pollutants.[43-45] Although superior photocatalytic performance can be improved for the hierarchically ZnO mircostructured, to our knowledge, there are rare research reports on enhanced photocatalytic performance of hierarchical structured ZnO/CNTs composites.

In our recent works, we have fabricated hierarchical structured TiO_2/Ag microspheres using a facile chemical deposition route and applied in photocatalytic degradation of MB.[46] In this work, we further explore the application of this method in the one-step fabrication of novel hierarchical structured ZnO/CNTs microsphere composites for photocatalytic degradation of MB. The novel hierarchical ZnO/CNTs microsphere composite with 1.1 wt% CNTs achieves a maximum degradation efficiency of 92.3% and 76% under UV and visible light irradiation for 60 min, compared with pure ZnO microspheres (70.4% and 37%), respectively. The enhanced photocatalytic performance is attributed to the triple effects of high surface area, enhanced light absorption and suppression of charge carriers recombination resulting from the interaction between ZnO and CNTs.

2. Experimental

The hierarchical ZnO/CNTs microspheres were obtained by a facile sol-gel hydrothermal method.[47] In brief, different amounts of multi-walled CNTs (Shenzhen Nanotech Port Co., Ltd., China), 0.8 g of zinc acetate ($Zn(CH_3COO)_2$) and 0.6 g of citric acid ($C_6H_8O_7$) were placed in the 50 mL distilled water, and then 10 mL of absolute ethyl alcohol (C_2H_6O) was added to the above mixture to keep the stirring well. Then 20 mL of 1 mol/L NaOH solution was gradually added to the above solution under stirring. The mixed solution was transferred into a 100 ml autoclave and heated at 120 ^oC for 24 h, and then cooled to room temperature naturally. And then above solution was washed with distilled water and absolute ethyl alcohol (C_2H_6O). Finally, as-prepared microspheres were obtained by vacuum drying at 60 ^oC for 24 h. In this work, the as-prepared hierarchical ZnO/CNTs microsphere composites with 0, 0.8, 1.1, 1.5 and 2.3 wt% were named as ZC-0, ZC-0.8, ZC-1.1, ZC-1.5 and ZC-2.3, respectively.

The morphology and structure of as-prepared samples were characterized by an scanning electronic microscopy (SEM, HATICH 4800), a JEOL-2010 high-resolution transmission electron microscope (HRTEM), X-ray diffraction (XRD, Japan MAC Science Co.), and Raman spectrometer (HORIBA Scientific) with an excitation of 532 nm laser light, respectively. The UV-vis absorption spectra of as-prepared samples were detected using a UV-vis spectrophotometer (Hitachi U-3900). Photoluminescence (PL) spectra were recorded on a HORIBA Jobin Yvon fluoromax-4 fluorescence spectrophotometer, using the 350 nm excitation line of a Xe lamp as light source. Brunauer-Emmett-Teller (BET) surface area was measured by ASAP 2020 Accelerated Surface Area and Porosimetry System (Micrometitics, Norcross, GA).

The photocatalytic activities of as-prepared samples were evaluated via decomposing methylene blue (MB) dye solution at room temperature. The concentration of MB and photocatalyst were set as 30 mg/L and 0.17g/L, respectively. Prior to irradiation, the suspensions were magnetically stirred in the dark for 30 min to establish an adsorption/desorption equilibrium. The dispersions were kept under constant air-equilibrated conditions before and during irradiation. The photocatalytic degradation process was observed by the change of the absorbance maximum in optical absorption spectra of MB dye. A 500W Hg lamp and 500w Xe lamp equipped with a 420 nm cutoff filter were employed as UV and visible light sources, and located 20 cm away from the reactor to trigger the photocatalytic reaction, respectively. A certain volume of suspension were drawn at selected times for analysis. The absorbance spectra of the temporal variations of the MB dye were recorded by a Shimadzu UV-3310 spectrometer.

3. Results and discussion

Figure 1 a and b show the FESEM images of as-prepared pure ZnO (ZC-0) and ZnO/CNTs (ZC-1.1) hierarchical composite microspheres, respectively. It can be observed that as-prepared microspheres are composed of self-assembled radial nano-flakes, and these microspheres display three-dimensional hierarchical morphology with a average size of about 2 ± 0.2 μm. The FESEM image of as-prepared ZnO/CNTs microsphere composites is shown in Figure 1 c. Compared with pure ZnO microspheres, it can be observed that these ZnO mircospheres are well wrapped around by the CNTs. Figure 1 d is magnified FESEM image of the black pane area marked in Figure 1c, showing the integration between ZnO nano-flakes and CNTs, which further confirms the formation of hierarchical ZnO/CNTs 3D structure with a good connect between ZnO and CNTs. The composition of as-prepared ZC-1.1 composite was identified by energy dispersive X-ray spectroscopy (EDS) linked to FESEM, as shown in Figure 2. The results display that the main elements such as C, Zn and O are present with no unexpected elements being observed, and the atomic ratios of C, ZnO and O in composite are 29, 56 and 15 %, respectively, indicating the purity of as-prepared samples.

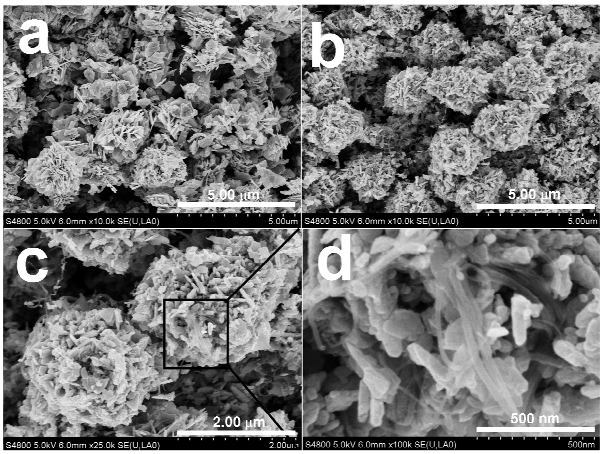

Figure 1 FESEM images of (a) ZC-0 mircospheres, (b) and (c) ZC-1.1 composite, and (d) magnified image of the black pane area in (c).

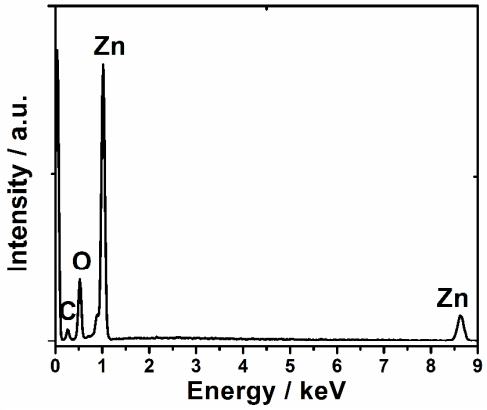

Figure 2 EDX spectrum of as-prepared ZC-1.1 composite.

The high-resolution transmission electron microscope (HRTEM) images of as-prepared ZC-1.1 composite are shown in Figure 3. The synthesized composite show a nearly mono-dispersed spherical shape with sizes of ca 2 μm (as shown in Figure 3 a and b). Figure 3 c and d show that the high-magnification HRTEM images of as-prepared ZC-1.1 composite. The crystallites connecting to the CNTs have a lattice fringe of 0.28 nm which is ascribed to the (1 0 0) plane of ZnO (JCPDS 36-1451).

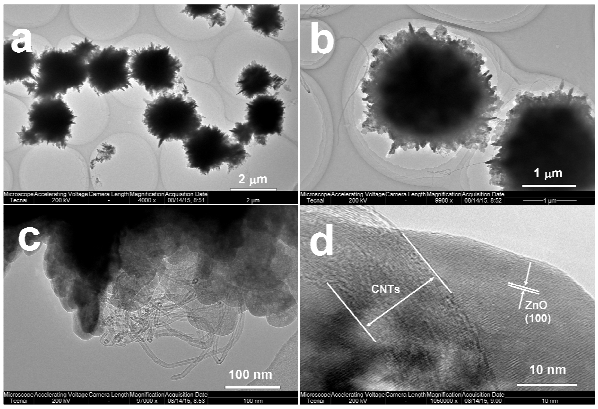

Figure 3 HRTEM images of as-prepared ZC-1.1 composite.

The XRD patterns of as-prepared ZC-0, ZC-0.8, ZC-1.1, ZC-1.5 and ZC-2.3 are shown in Figure 4. The characteristic diffraction peaks at 31.8°, 34.4°, 36.3°, 47.5°, 56.6°, 62.9°, 66.6°, 68.1°, and 69.2° are indexed to (100), (002), (101), (102), (110), (103), (200), (112) and (201) crystal planes of the wurtzite-structure (JPCDS 36-1451) of ZnO, which demonstrates that the presence of CNTs does not result in the development of new crystal orientations or changes in preferential orientations of ZnO. The XRD analysis further shows that the main diffraction peaks of ZnO/CNTs composites are similar to those of pure ZnO, which demonstrates that the presence of CNTs does not result in the development of new crystal orientations or changes in preferential orientations of ZnO. It is noted that no typical diffraction peaks of carbon species are observed, which may be due to the low amount and relatively low diffraction intensity of CNTS in the composites.[48]

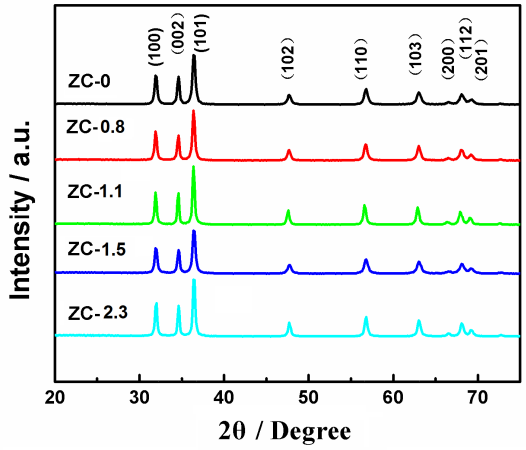

Figure 4 XRD patterns of as-prepared ZC-0, ZC-0.8, ZC-1.1, ZC-1.5, and ZC-2.3 composites.

The Raman spectra of as-prepared ZC-0 and ZC-1.1 are shown in Figure 5. The pure ZnO exhibits a strong Raman peak at 435 cm^{-1} corresponds to E2 mode of ZnO crystal. A small peaks at 326 cm^{-1} is assigned to zoneboundary phonons 3E2H–E2L for wurtzite ZnO single crystals which is matched up with Raman peak of bulk ZnO crystals.[49] In addition,a longitudinal-optical (LO) mode at 573 cm^{-1}, together with its overtones at 1146 cm^{-1} are observed for pure ZnO mircospheres. Compared with pure ZnO, characteristic D peak at 1343 cm^{-1} and G peak at 1575 cm^{-1} are observed for ZC-1.1 composite. The G peak is the response of the in-plane stretching motion of symmetric sp^2 C-C bonds, whereas the D peak results from the disruption of the symmetrical hexagonal graphitic lattice.[50] This results further confirm that ZnO/CNTs composites have been prepared by the facile chemical deposition method.

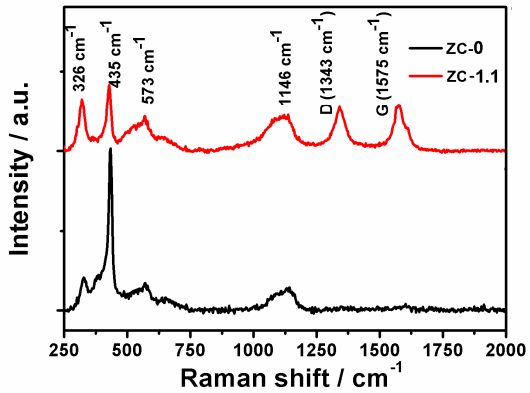

Figure 5 Raman spectra of as-prepared ZC-0 and ZC-1.1 microsphere composites.

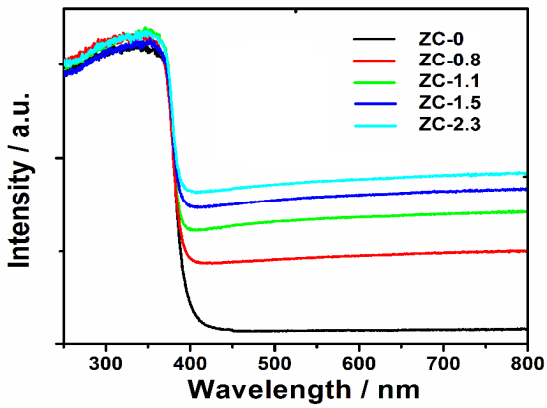

Figure 6 UV-vis absorption spectra of as-prepared ZC-0, ZC-0.8, ZC-1.1, ZC-1.5, and ZC-2.3 composites.

The UV-vis absorption spectra of ZC-0, ZC-0.8, ZC-1.1, ZC-1.5 and ZC-2.3 composites are displayed in Figure 6. The absorption edges are derived from the intersection of the sharply decreasing region of a spectrum.[51] Compared to the absorption edge of pure ZnO (ca 400 nm), there is not a obvious change for the composites. The band gaps of the pure ZnO and composites obtained from the absorption edge are about 3.1 eV. Because ZnO and CNTs in the ZnO/CNTs composite are different two phases, their band-gap energies are not changed.[53] However, compared with pure ZnO, the visible light absorption of ZnO/CNTs composites gradually increases with the increase of CNTs content in the composites, which can be ascribed to the the

presence of the black CNTs.[54] The enhanced light absorption can increase the number of photo-generated electrons and holes to participate in the photocatalytic reaction and improve the photocatalytic performance.

The photoluminescence (PL) emission spectra of of ZC-0, ZC-0.8, ZC-1.1, ZC-1.5 and ZC-2.3 composites are shown in Figure 7. The results display that a broad emission band in the range of 380-650 nm, which is ascribed to luminescence from localized surface states due to recombination of photogenerated electron-hole pairs.[55] The PL intensity decreases with the increase of CNTs content, suggesting that the introduction of CNTs could quench the fluorescence from ZnO. The quenching mechanism of the PL spectra may because electron transfers from the excited ZnO.[56] It may be possible to increase electron transfer and interfacial interaction between ZnO and CNTs, and reduce the electron-hole pair recombination, which can increase the photocatalytic activity. However, ZG-2.3 exhibits a significant increase of intensity compared to that of other composites, which is because that the excessive CNTs on ZnO can act as a kind of recombination center instead of providing an electron pathway.[57,58]

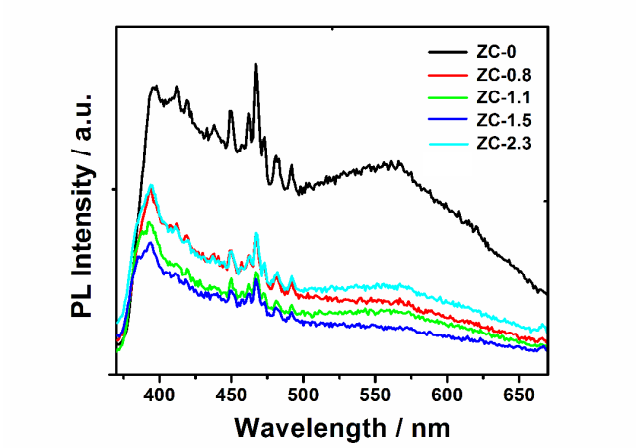

Figure 7 Room-temperature PL emission spectra of as-prepared ZC-0, ZC-0.8, ZC-1.1, ZC-1.5, and ZC-2.3 composites.

The photocatalytic degradation of MB under UV and visible light irradiation is used to evaluate the photocatalytic performance of as-prepared pure ZnO and ZnO/CNTs composites. Figure 8a shows the absorption spectrum of MB using as-prepared ZC-1.1 composite with reaction time under UV light radiation, which indicates that the MB content decreases with the increase of the light irradiation time. Figure. 8b shows the photocatalytic performance of as-prepared pure ZnO and ZnO/CNTs composites under UV light irradiation. The normalized temporal concentration changes (C/Co) of MB during photodegradation are propor-tional to the normalized maximum absorbance (A/Ao). The photocatalytic activity of as-prepared ZC-0.8 composites (72.8%) is higher than that of pure ZnO (ZC-0) (70.4%). When CNTs amount is increased, the degradation efficiency is increased, and reaches a maximum value of 92.3% for ZC-1.1. However, when the CNTs loading is further increased, the photocatalytic performance will decrease, which is due to the following two reasons: (1) light harvesting competition between CNTs and ZnO appears with increase of CNTs amount,[53] (2) the excessive CNTs can act as a kind of recombination center instead of providing an electron pathway.[57,58] The photocatalytic performance of as-prepared pure ZnO and ZnO/CNTs composites under visible light irradiation indicates a similar trend as the photocatalytic degradation of MB under UV light irradiation (as shown in Figure 8c). Under visible irradiation, the photocatalytic activity of as-prepared ZC-1.1 composite reaches a maximum value of 76%. According to above results, the enhanced photocatalytic performance of as-prepared ZnO/CNTs composites suggests that the introduction of CNTs play an important role in the photocatalytic performance. The stability of as-prepared composite with ZC-1.1 as catalyst under UV light irradiation is also studied (as shown in Figure. 8d). It can be seen that the photocatalytic activity of composite do not decrease conspicuously after six successive cycles of degradation tests, indicating that this composite is fairly stability.

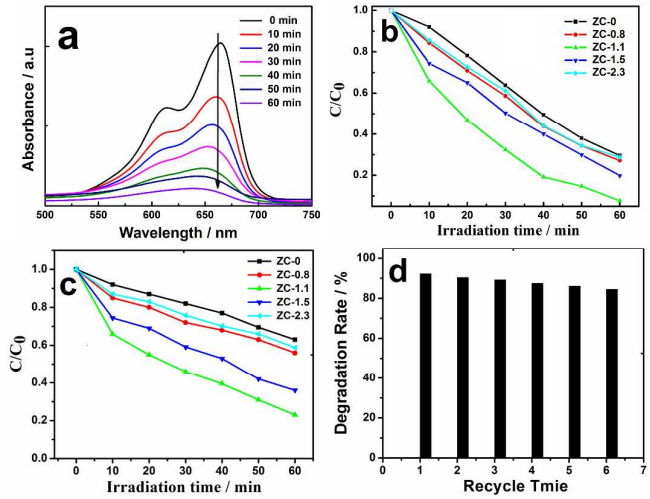

Figure 8 (a) UV-vis absorption spectra of degradation MB solution over ZC-1.1 under UV light irradiation, photocatalytic degradation of MB in the presence of as-prepared ZC-0, ZC-0.8, ZC-1.1, ZC-1.5, and ZC-2.3 composites under (b) UV and (c) visible light irradiation, and (d) recycle photocatalytic degradation performance of ZC-1.1 under UV light irradiation.

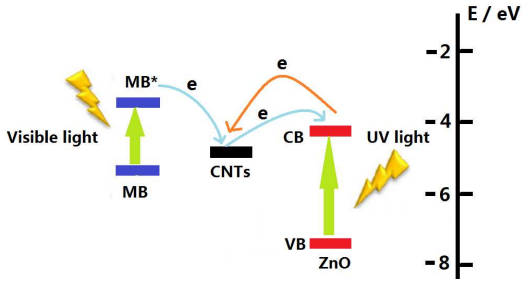

Figure 9 Schematic diagram of energy levels of excited MB, CNTs and ZnO.

Based on the experimental results, the higher photocatalytic activity of ZnO/CNTs composites could be summarized as follows: (1) Higher surface area. The BET surface area of as-prepared ZC-0 and ZC-1.1 was carried out, and the results indicate that the surface area of ZC-1.1 (26.1 m^2g^{-1}) is higher than than that of pure ZnO (17.6 m^2g^{-1}) due to loading CNTs with higher surface area. The higher surface areas result in the large contact areas between the active sites and the target substrate, which can increase the photocatalytic activity. (2) Increased visible light absorption. The strong absorption of visible light can be produced due to the introduction of CNTs (as shown in Figure 6), which increases the number of photo-generated electrons and holes to participate in the photocatalytic reaction and improve the photocatalytic performance. (3) the reduced electron-hole pair recombination and increased electron transfer. The photocatalytic degradation of MB by ZnO/CNTs composites under light irradiation involves two mechanisms. The work function of excited MB, CNTs, and conduction band (CB) of ZnO are -3.60, -4.80eV and -4.05eV (vs. Vacuum)[52,59], respectively, as shown in Figure 9. Under the UV light irradiation, the electrons are excited from the valence band (VB) of ZnO to CB, and then these photo-induced electrons transfer from the CB of ZnO to CNTs. On the other hand, the dye can acts as a sensitizer of visible light, and excited electrons transfer to the CB of ZnO via CNTs. In the whole electron transfer process, CNTs could efficiently increase electron transfer and reduce the lectron-hole pair recombination[60,61], which is confirmed by the results from PL emission spectra (as shown in Figure 7), leading to a enhanced photocatalytic performance.

4. Conclusions

In summarized, the novel ZnO/CNTs hierarchical mircosphere composites have been prepared for photocatalytic degradation of MB under UV and visible light irradiation. The results show that the photocatalytic activity of ZnO/CNTs composites is superior to that of pure ZnO mircospheres, and as-prepared ZnO/RGO composite with 1.1 wt.% CNTs achieves a maximum degradation efficiency under and visible light irradiation. The enhanced photocatalytic performance is ascribed to the triple effects of high surface area, enhanced light absorption and suppression of charge carriers recombination resulting from the interaction between ZnO and CNTs.

Acknowledgment

This work is supported by the National Science Foundation of China (NSFC) (21271136), the Provincial Natural Science Foundation of Anhui (1508085ME104 and 1408085MB40), the Scientific Research Foundation for the Anhui Provincial Returned Overseas Chinese Scholars (Electrospun low dimensional TiO_2 nano-structures and application in photovoltaic devices), the Important Project of Anhui Provincial Education Department (KJ2011A260) and the Program of Innovative Research Team of Suzhou University (2013kytd02), the Scientific Research Foundation of Suzhou University (2014XQNRL012).

Notes and references

1 Anhui Key Laboratory of Spin Electron and Nanomaterials, Suzhou University, Suzhou 234000, P. R. China, Tel.: +86-557-2871006; Fax: +86-557-2871003; E-mail: Prof. L. Zhang zhlisuzh@163.com; Prof. G. Zhu guangzhu@ahsztc.edu.cn.

[2]Department of Materials Science and Engineering, Northwestern University, Evanston, Illinois, 60208, United States

1. A. Fujishima and K. Honda, *Nature*, 1972, **238**, 37.
2. M. R. Hoffmann, S. T. Martin, W. Choi and D. W. Bahnemann, *Chem. Rev*., 1995, **95**, 69.
3. J. L. Yang, S. J. An, W. I. Park, G. C. Yi and W. Choi, *Adv. Mater*., 2004, **16**, 1661.
4. S. Rehman, R. Ullah, A. M. Butt and N. D. Gohar, *Hazard, J. Mater*., 2009, **170**, 560.
5. L. P. Xu, Y. L. Hu, C. Pelligra, C. H. Chen, L. Jin, H. Huang, S. Sithambaram, M. Aindow, R. Joesten and S. L. Suib, *Chem. Mater*., 2009, **21**, 2875.
6. X. Chen, L. Liu, Y. Y. Peter and S. S. Mao, *Science*, 2011, **331**, 746.
7. X. Liu, L. Pan, Q. Zhao, T. Lv, G. Zhu, T. Chen, T. Lu, Z. Sun and C. Sun, *Chem. Eng. News*., 2012, **183**, 238.
8. X. Y. Li, F. F. Wang, Q. R. Qian, X. P. Liu, L. R. Xiao and Q. H. Chen, *Mater. Lett.*, 2012, **66,** 370.
9. L. K. Pan, X. J. Liu, Z. Sun and C. Q. Sun, *J. Mater. Chem. A*, 2013, **1**, 8299.
10. X. Xu, C. Randorn, P. Efstathiou and J. T. Irvine, *Nat. Mater*., 2012, **11**, 595.
11. D. Ravelli, D. Dondi, M. Fagnoni and A. Albini, *Chem. Soc. Rev*., 2009, **38**, 1999.
12. M. D. Tzirakis, I. N. Lykakis and M. Orfanopoulos, *Chem. Soc. Rev*., 2009, **38**, 2609.
13. T. Wu, G. Liu, J. Zhao, H. Hidaka and N. V. Serpone, *J. Phys. Chem. B*, 1998, **102**, 5845.
14. J. Yu, G. Dai and B. Huang, *J. Phys. Chem. C*, 2009, **113**, 16394.
15. X.J. Liu, L. K. Pan, T. Lv, G. Zhu, Z. Sun and C. Sun, *Chem. Commun*., 2011, **47**, 11984.
16. C. X. Guo, H. B. Yang, Z. M. Sheng, Z. S. Lu, Q. L. Song and C. M. Li, *Angew. Chem. Int. Ed*., 2010, **49**, 3014.
17. M. Xiao, L. Wang, Y. Wu, X. Huang and Z. Dang, *Nanotechnology*, 2008, **19**, 015706.
18. Y. Wen, B. Liu, W. Zeng and Y. Wang, *Nanoscale*, 2013, **5**, 9739.
19. X. J. Liu, L. K. Pan, T. Lv, Z. Sun and C. Sun, *RSC Advances*, 2012, **2**, 3823
20. M. Xing, Y. Wu, J. Zhang and F. Chen, *Nanoscale*, 2010, **2**, 1233.
21. H. Zhang, C. Liang, J. Liu, Z. Tian, G. Wang and W. Cai, *Langmuir*, 2012, **28**, 3938.
22. W. Lu, G. Liu, S. Gao, S. Xing and J. Wang, *Nanotechnology*, 2008, **19**, 445711.
23. S. Liu, L. Yang, S. Xu, S. Luo and Q. Cai, *Electrochem. Commun*., 2009, **11**, 1748.
24. S. Fukuzumi and T. Kojima, *J. Mater. Chem.*, 2008, **18**, 1427.
25. G. Zhu, L. K. Pan, T. Lu, T. Xu and Z. Sun, *J. Mater. Chem*., 2011, **21**, 14869.
26. O. Akhavan, R. Azimirad, S. Safad and M. M. Larijani, *J. Mater. Chem.*, 2010, **20**, 7386.
27. W. J. Lee, M. L. Ju, S. T. Kochuveedu, T. H. Han, Y. J. Hu and M. Park, *Acs Nano*, 2011, **6**, 935.

28. J. Zhong, F. Chen and J. L. Zhang, *J. Phys. Chem. C*, 2010, **114**, 933.
29. T. S. Jiang, L. Zhang, M. R. Ji, Q. Wang, Q. Zhao, X. Q. Fu and H. B. Yin, *Particuology*, 2013, **11**, 737.
30. L. C. Chen, Y. C. Ho, W. S. Guo, C. M. Huang and T. C. Pan, *Electrochim. Acta*, 2009, **54**, 3884.
31. M. Ahmad, E. Ahmed, Z. L. Hong, X. L. Jiao, T. Abbas and N. R. Khalid, *Appl. Surf. Sci*., 2013, **285**, 702.
32. M. Q. Yang, N. Zhang, and Y. J. Xu, *ACS Appl. Mater. Inter*., 2013, **5**, 1156.
33. T. C. An, J. Y. Chen, X. N. Nie, G. Y. Li, H. M. Zhang, X. L. Liu and H. J. Zhao, *ACS Appl. Mater. Inter*, 2012, **4**, 5988.
34. K. Woan, G. Pyrgiotakis and W. Sigmund, *Adv. Mater*. 2009, **21**, 2233.
35. Y. J. Xu, Y. B. Zhuang and X. Z. Fu, *J. Phys. Chem. C*, 2010, **114**, 2669.
36. R. Leary, A. Westwood, R. Leary and A. Westwood, *Carbon*, 2011, **49**, 741.
37. K. Ouyang, S. Xie and X. Ma, *Ceram. Int*., 2013, **39**, 7531.
38. J. G. Yu, T. T. Ma and S. W. Liu, Phys. *Chem. Chem. Phys.*, 2011, **13**, 3491.
39. T. P. Chou, Q. F. Zhang, G. E. Fryxell and G. Z. Cao, *Adv. Mater*., 2007, **19**, 2588.
40. G. Z. Cao, K. Park, Q. F. Zhang, B. B. Garcia, X. Y. Zhou and Y. H. Jeong, *Adv. Mater*., 2010, **22**, 2329.
41. T. Lv, L. K. Pan, X. J. Liu and Z. Sun, *Catal. Sci. Technol.*, 2012, **2**, 2297.
42. L. Jiang and L. Gao, *Mater. Chem. Phys*., 2005, **91**, 313.
43. H. B. Lu, S. M. Wang, L. Zhao, J. C. Li, B. H. Dong and Z. X. Xu, J. *Mater. Chem.*, 2011, **21**, 4228.
44. F. Xu, Y. T. Shen, L. T. Sun, H. B. Zeng and Y. N. Lu, *Nanoscale*, 2011, **3**, 5020.
45. X. Zhang and F. Q. Shi, *J. Inter. Nanosci*., 2014, **13**, 1450023.
46. L. Zhang, L. Chen, L. W. Chen and G. Zhu, *RSC Advances*, 2014, **4**, 54463.
47. Y. Zhang and J. C. Mu, *Nanotechnol.*, 2007, **18**, 075606.
48. Y. L. Chen, Z. A. Hu, Y. Q. Chang, H. W. Wang, Z. Y. Zhang, Y. Y. Yang and H. Y. Wu, *J. Phys. Chem. C*, 2011, **115**, 2563.
49. C. Roy, S. Byrne, E. McGlynn, J. P. Mosnier, E. D. Posada, D. O'Mahony, J. G. Lunney, M. O. Henry, B. Ryan and A. A. Cafolla, *Thin Solid Films*, 2003, **436**, 273.
50. N. J. Bell, Y. H. Ng, A. Du, H. Coster, S. C. Smith and R. Amal, *J. Phys. Chem. C*, 2011, **115**, 6004.
51. S. Banerjee, S. K. Mohapatra, P. P. Das and M. Misra, *Chem. Mater.*,2008, **20** 6784.
52. Y. Yao, G. Li, S. Ciston, R. M. Lueptow and K. A. Gray, *Environ. Sci. Technol.*, 2008, **42**, 4952.
53. T. G. Xu, L.W. Zhang, H.Y. Cheng and Y.F. Zhu, *Appl. Catal. B*, 2011, **101**, 382.
54. B. X. Li, T. X. Liu, Y. F. Wang and Z. F. Wang, *J. colloid. Interf. Sci.*, 2012, **377**, 114.
55. Z. Chen, S. Berciaud, C. Nuckolls, T. F. Heinz and L. E. Brus, *ACS Nano,* 2010, **4** , 2964.
56. Y. H. Zhang, Z. R. Tang, X. Z.Fu and Y. J. Xu, *ACS Nano,* 2010, **4**, 7303.
57. G. Zhu, T. Xu, T. Lv, L. Pan, Q. Zhao and Z. Sun, *J. Electroanal. Chem*., 2011, **650**, 248.
58. N. Yang, J. Zhai, D. Wang, Y. Chen and L. Jiang, *ACS Nano*, 2010, **4**, 887.
59. M. Ahmad, E. Ahmed, Z. L. Hong, J. F. Xu, N. R. Khalid, A. Elhissi and W. Ahmed, *Appl. Surf. Sci*., 2013, **274**, 273.
60. S. Sun, L. Gao and Y. Liu, *Appl. Phys. Lett*., 2010, **96**, 083113.
61. E. Gao, W. Wang, M. Shang and J. Xu, *Phys. Chem. Chem. Phys*., 2011, **13**, 2887.